

1 Autocorrelation function of velocity increments 2 time series in fully developed turbulence

3 Y.X. HUANG^{1,2}, F. G. SCHMITT² ^(a), Z.M. LU¹ and Y.L. LIU¹

4 ¹ Shanghai Institute of Applied Mathematics and Mechanics, Shanghai University, 200072
5 Shanghai, China

6 ² Université des Sciences et Technologies de Lille - Lille 1, CNRS, Laboratory of Oceanology
7 and Geosciences, UMR 8187 LOG, 62930 Wimereux, France, EU

8
9
PACS 05.45.Tp – Time series analysis
PACS 02.50.Fz – Stochastic analysis
PACS 47.27.Gs – Isotropic turbulence; homogeneous turbulence

10 **Abstract.** - In fully developed turbulence, the velocity field possesses long-range correlations,
11 denoted by a scaling power spectrum or structure functions. Here we consider the autocorrelation
12 function of velocity increment $\Delta u_\ell(t)$ at separation **distance time** ℓ . Anselmet et al. [Anselmet
13 et al. J. Fluid Mech. **140**, 63 (1984)] have found that the autocorrelation function of velocity
14 increment has a minimum value, whose location is approximately equal to ℓ . Taking statistical
15 stationary assumption, we link the velocity increment and the autocorrelation function with the
16 power spectrum of the original variable. We then propose an analytical model of the autocorrelation
17 function. With this model, we prove that the location of the minimum autocorrelation function is
18 exactly equal to the separation **scale time** ℓ when the scaling of the power spectrum of the original
19 variable belongs to the range $0 < \beta < 2$. This model also suggests a power law expression for the
20 minimum autocorrelation. Considering the cumulative function of the autocorrelation function, it
21 is shown that the main contribution to the autocorrelation function comes from the large scale part.
22 Finally we argue that the autocorrelation function is a better indicator of the inertial range than
23 the second order structure function.

24
25 **Introduction.** – Turbulence is characterized by power law of the velocity spectrum [1]
26 and structure functions in the inertial range [2,3]. This is associated to long-range power-law
27 correlations for the dissipation or absolute value of the velocity increment. Here we consider
28 the autocorrelation of velocity increments (without absolute value), inspired by a remark
29 found in Anselmet et al. (1984) [4]. In this reference, it is found that the location of the
30 minimum value of the autocorrelation function $\Gamma(\tau)$ of velocity increment $\Delta u_\ell(t)$, **defined**
31 **as**

$$\Delta u_\ell(t) = u(t + \ell) - u(t) \quad (1)$$

32 of fully developed turbulence with **distance time** separation ℓ is approximately equal to ℓ .
33 The autocorrelation function of **this time series** is defined as

$$\Gamma(\tau) = \langle (V_\ell(t) - \mu)(V_\ell(t - \tau) - \mu) \rangle \quad (2)$$

^(a)E-mail: francois.schmitt@univ-lille1.fr

34 where $V_\ell(t) = \Delta u_\ell(t)$, μ is the mean value of $V_\ell(t)$, and $\tau > 0$ is the time lag.

35 This paper mainly presents analytical results. In first section we present the database
 36 considered here as an illustration of the property which is studied. The next section presents
 37 theoretical studies. The last section provides a discussion.

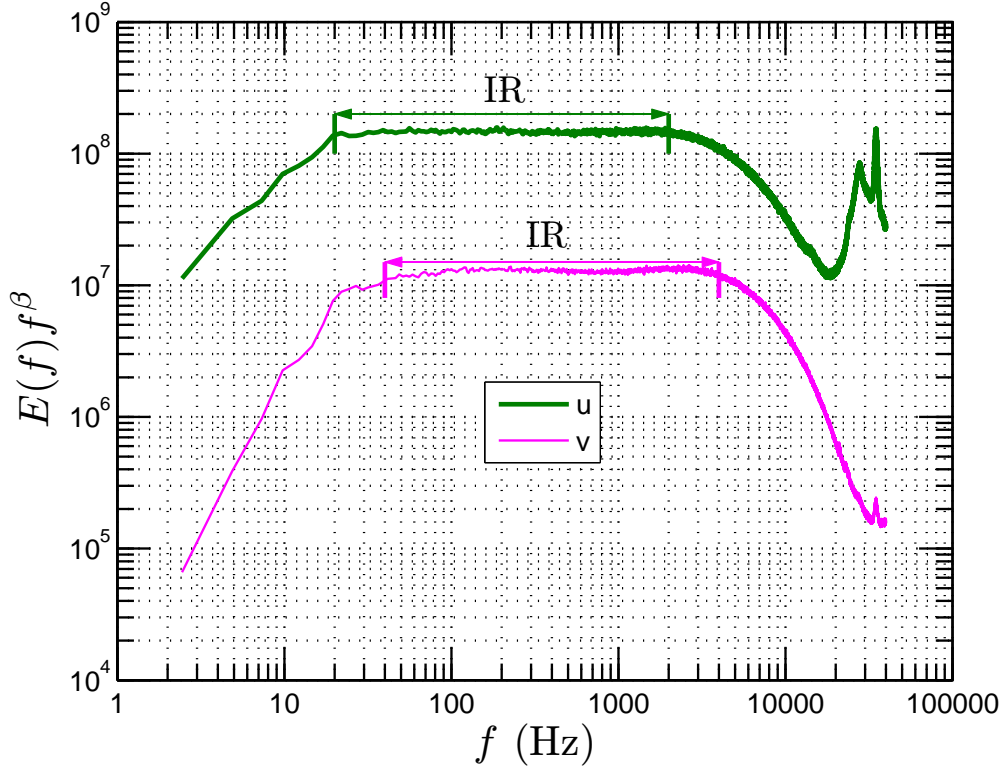


Fig. 1: Compensated spectrum $E(f)f^\beta$ of **streamwise (longitudinal)** ($\beta \simeq 1.63$) and **spanwise (transverse)** ($\beta \simeq 1.62$) velocity, where β is the corresponding power law estimated from the power spectrum. The plateau is observed on the range $20 < f < 2000$ Hz and $40 < f < 4000$ Hz for **streamwise (longitudinal)** and **spanwise (transverse)** velocity, respectively.

38 **Experimental analysis of the autocorrelation function of velocity increments.**

39 – We consider here a turbulence velocity time series obtained from an experimental ho-
 40 mogeneous and nearly isotropic turbulent flow at downstream $x/M = 20$, where M is the
 41 mesh size. The flow is characterized by the Taylor microscale based Reynolds number
 42 $Re_\lambda = 720$ [5]. The sampling frequency is $f_s = 40$ kHz and a low-pass filter at a frequency
 43 20 kHz is applied to the experimental data. The sampling time is 30 s, and the number
 44 of data points per channel for each measurement is 1.2×10^6 . We have 120 realizations
 45 with four channels. The total number of data points at this location is 5.76×10^8 . The
 46 mean velocity is 12 ms^{-1} . The rms velocity is 1.85 and 1.64 ms^{-1} for streamwise (longi-
 47 tudinal) and spanwise (transverse) velocity component. The Kolmogorov scale η and the
 48 Taylor microscale λ are 0.11 mm and 5.84 mm respectively. Let us note here $T_s = 1/f_s$ the
 49 time resolution of these measurements. This data demonstrates an inertial range over two
 50 decades [5], see a compensated spectrum $E(f)f^\beta$ in fig. 1, where $\beta \simeq 1.63$ and $\beta \simeq 1.62$
 51 for **streamwise (longitudinal)** and **spanwise (transverse)** velocity respectively. We show the
 52 autocorrelation function $\Gamma_\ell(\tau)$ directly estimated from these data in fig. 2. Graphically, the
 53 location τ_o of the minimum value of each curve is very close to ℓ , which confirms Anselmet's

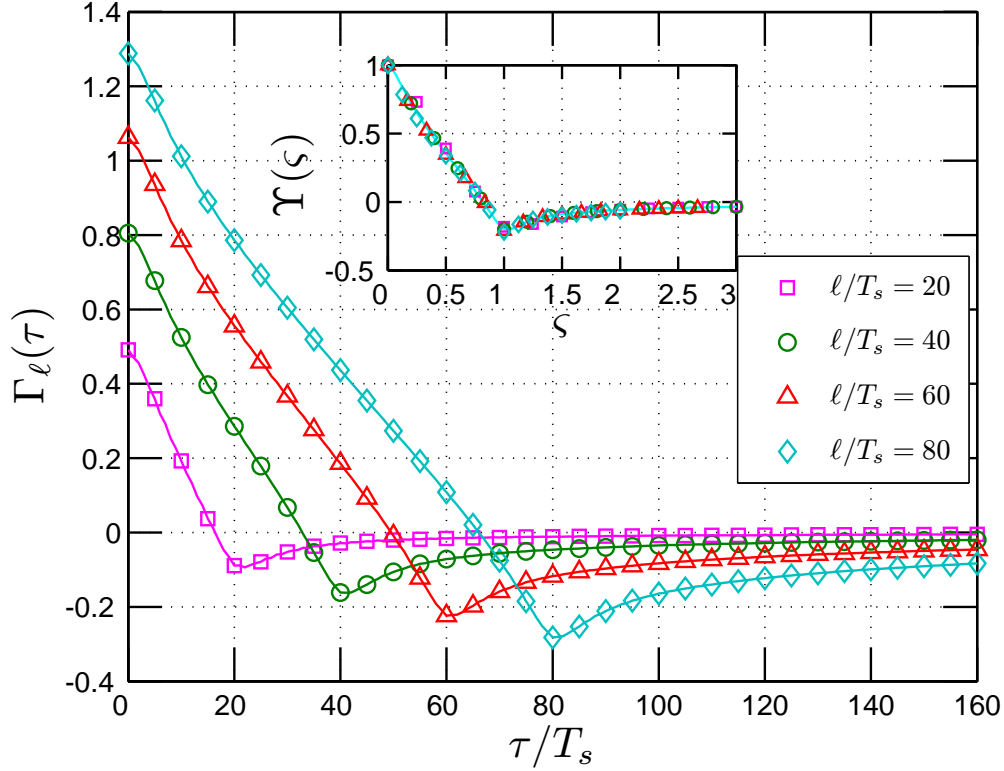


Fig. 2: Autocorrelation function $\Gamma_\ell(\tau)$ of the velocity increment $\Delta u_\ell(t)$ estimated from an experimental homogeneous and nearly isotropy turbulence time series with various increments ℓ . The location of the minimum value is very close to the separation **scale time** ℓ . The inset shows the rescaled autocorrelation function $\Upsilon(\xi)$.

54 observation [4]. Let us define

$$\Gamma_o(\ell) = \min_{\tau} \{\Gamma_\ell(\tau)\} \quad (3)$$

55 and τ_o the location of the minimum value

$$\Gamma_o(\ell) = \Gamma_\ell(\tau_o(\ell)) \quad (4)$$

56 We show the estimated $\tau_o(\ell)$ on the range $2 < \ell/T_s < 40000$ in fig. 3, where the inertial
 57 range is indicated by IR. It shows that when ℓ is greater than $20T_s$, τ_o is very close to ℓ even
 58 when ℓ is in the forcing range, in agreement with the remark of Anselmet et al. [4]. In the
 59 following, we show this analytically.

60 **Autocorrelation function.** – Considering the statistical stationary assumption [3],
 61 we represent $u(t)$ in Fourier space, which is written as

$$\hat{U}(f) = \mathcal{F}(u(t)) = \int_{-\infty}^{+\infty} u(t) e^{-2\pi i f t} dt \quad (5)$$

62 where \mathcal{F} means Fourier transform and f is the frequency. Thus, the Fourier transform of
 63 the velocity increment $\Delta u_\ell(t)$ is written as

$$S_\ell(f) = \mathcal{F}(\Delta u_\ell(t)) = \hat{U}(f)(e^{2\pi i f \ell} - 1) \quad (6)$$

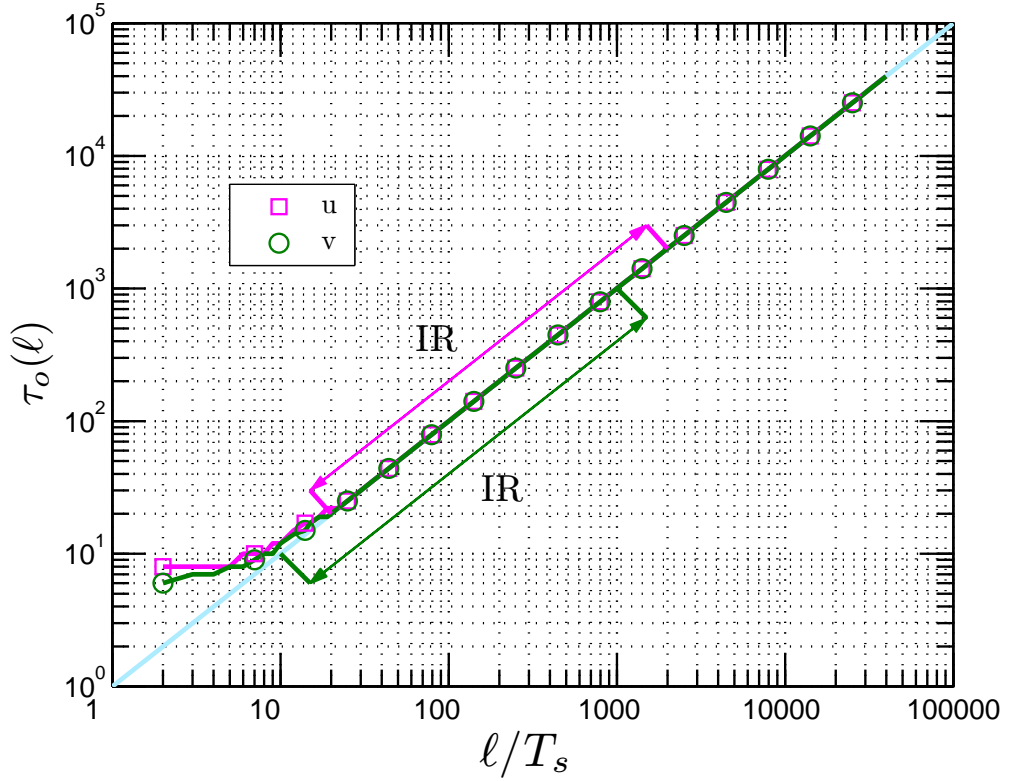


Fig. 3: Location $\tau_o(\ell)$ of the minimum value of the autocorrelation function estimated from experimental data, where the inertial range is marked as IR. The solid line indicates $\tau_o(\ell) = \ell$.

64 where $\Delta u_\ell(t) = u(t + \ell) - u(t)$. Hence, the 1D power spectral density function of velocity
 65 increments $E_\Delta(f)$ is expressed as

$$E_\Delta(f) = |S_\ell(f)|^2 = E_v(f)(1 - \cos(2\pi f\ell)) \quad (7)$$

66 where $E_v(f) = 2|\hat{U}(f)|^2$ is the velocity power spectrum [3]. It is clear that the velocity
 67 increment operator acts a kind of filter, where the frequencies $f_\Delta = n/\ell$, $n = 0, 1, 2, \dots$, are
 68 filtered.

69 Let us consider now the autocorrelation function of the increment. The Wiener-Khinchin
 70 theorem relates the autocorrelation function to the power spectral density via the Fourier
 71 transform [3, 6]

$$\Gamma_\ell(\tau) = \int_0^{+\infty} E_\Delta(f) \cos(2\pi f\tau) df \quad (8)$$

72 The theorem can be applied to wide-sense-stationary random processes, signals whose
 73 Fourier transforms may not exist, using the definition of autocorrelation function in terms
 74 of expected value rather than an infinite integral [6]. Substituting eq. (7) into the above
 75 equation, and assuming a power law for the spectrum (a hypothesis of similarity)

$$E_v(f) = cf^{-\beta}, \quad c > 0 \quad (9)$$

76 we obtain

$$\Gamma_\ell(\tau) = c \int_0^{+\infty} f^{-\beta} (1 - \cos(2\pi f\ell)) \cos(2\pi f\tau) df \quad (10)$$

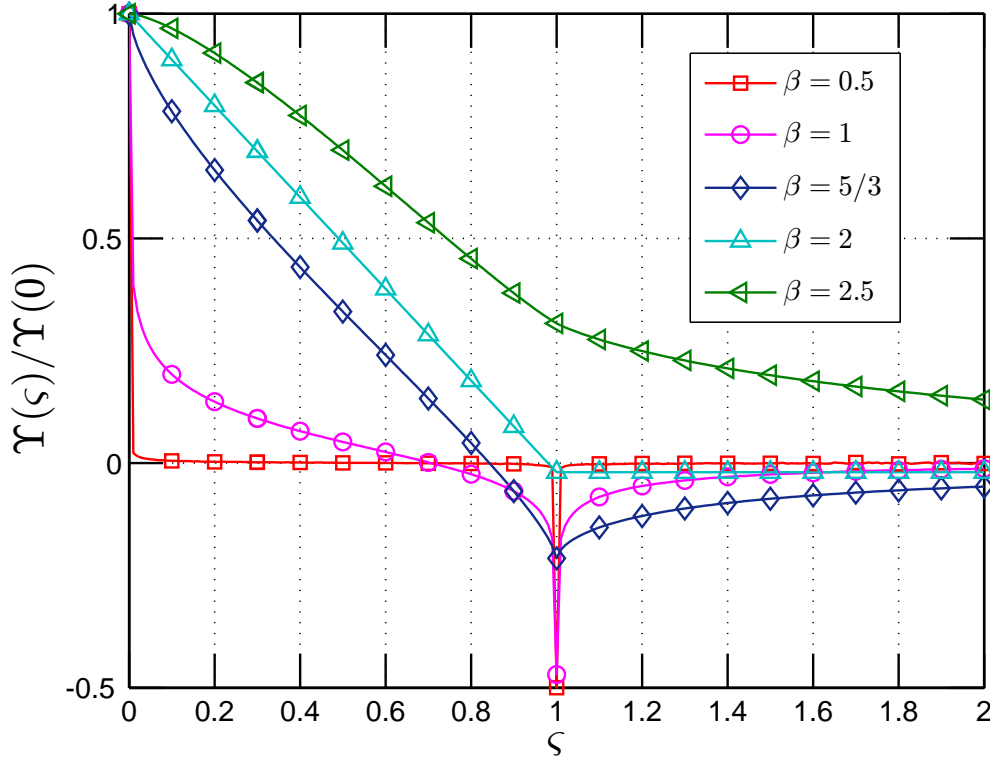


Fig. 4: Numerical solution of the rescaled autocorrelation function $\Upsilon(\varsigma)$ with various β from 0.5 to 2.5 estimated from eq. (10).

77 The convergence condition requires $0 < \beta < 3$. It implies a rescaled relation, using scaling
 78 transformation inside the integral. This can be estimated by taking $\ell' = \lambda\ell$, $f' = f\lambda$,
 79 $\tau' = \tau/\lambda$ for $\lambda > 0$, providing the identity

$$\Gamma_{\lambda\ell}(\tau) = \Gamma_{\ell}(\tau/\lambda)\lambda^{\beta-1} \quad (11)$$

80 If we take $\ell = 1$ and replace λ by ℓ , we then have

$$\Gamma_{\ell}(\tau) = \Gamma_1(\tau/\ell)\ell^{\beta-1} \quad (12)$$

81 Thus, we have a universal autocorrelation function

$$\Gamma_{\ell}(\ell\varsigma)\ell^{1-\beta} = \Upsilon(\varsigma) = \Gamma_1(\varsigma) \quad (13)$$

82 This rescaled universal autocorrelation function is shown as inset in fig. 2. A derivative of
 83 eq. (11) gives $\Gamma'_{\lambda\ell}(\tau) = \Gamma'_{\ell}(\tau/\lambda)\lambda^{\beta-2}$. The minimum value of the left-hand side is $\tau = \tau_o(\lambda\ell)$,
 84 verifying $\Gamma'_{\lambda\ell}(\tau_o(\lambda\ell)) = 0$ and for this value we have also $\Gamma'_{\ell}(\tau_o(\lambda\ell)/\lambda) = 0$. This shows that
 85 $\tau_o(\ell) = \tau_o(\lambda\ell)/\lambda$. Taking again $\ell = 1$ and $\lambda = \ell$, we have

$$\tau_o(\ell) = \ell\tau_o(1) \quad (14)$$

86 Showing that $\tau_o(\ell)$ is proportional to ℓ in the scaling range (when ℓ belongs to the inertial
 87 range). With the definition of $\Gamma_o(\ell) = \Gamma_{\ell}(\tau_o(\ell))$ we have, also using eq. (11), for $\tau = \tau_o(\lambda\ell)$:

$$\begin{aligned} \Gamma_{\lambda\ell}(\tau_o(\lambda\ell)) &= \Gamma_{\ell}(\tau_o(\lambda\ell)/\lambda)\lambda^{\beta-1} \\ &= \Gamma_{\ell}(\tau_o(\ell))\lambda^{\beta-1} \end{aligned} \quad (15)$$

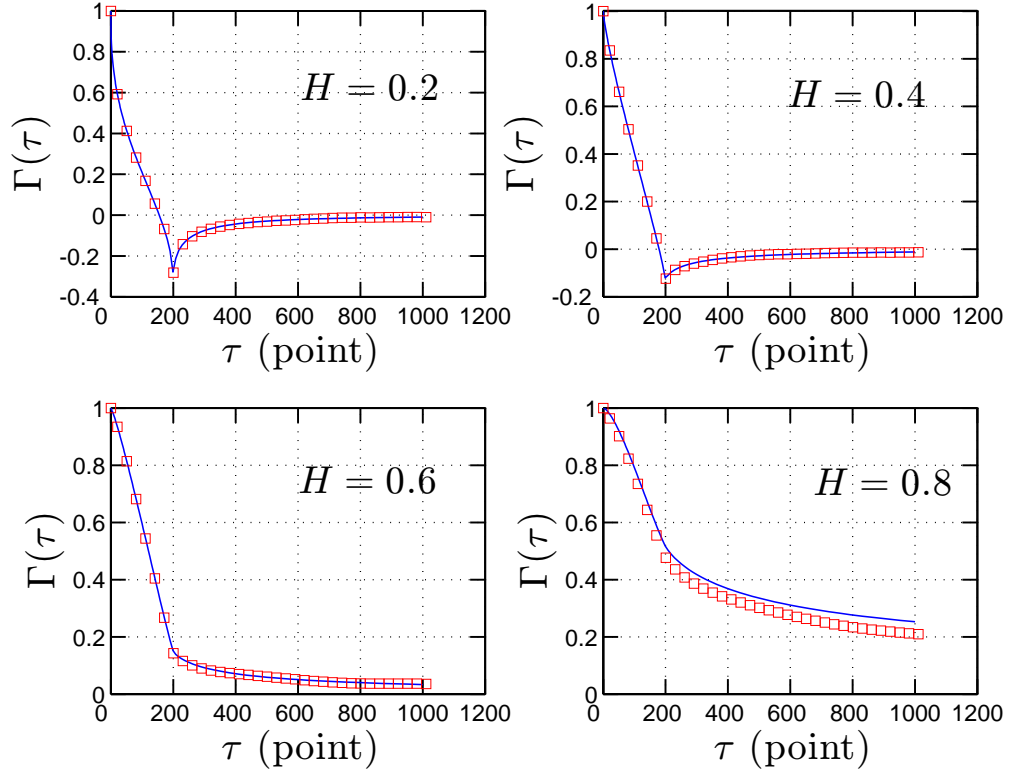


Fig. 5: Comparison of the autocorrelation function, which is predicted by eq. (20) (solid line) and estimated from fBm simulation (\square) with $\ell = 200$ points.

89 Hence $\Gamma_o(\lambda\ell) = \lambda^{\beta-1}\Gamma_o(\ell)$ or

$$\Gamma_o(\ell) = \Gamma_o(1)\ell^{\beta-1} \quad (16)$$

90 We now consider the location $\tau_o(1)$ of the autocorrelation function for $\ell = 1$. We take
91 the first derivative of eq. (10), written for $\ell = 1$

$$\mathcal{P}(\tau) = \frac{d\Gamma_1(\tau)}{d\tau} = - \int_0^{+\infty} f^{1-\beta}(1 - \cos(2\pi f)) \sin(2\pi f\tau) df \quad (17)$$

92 where we left out the constant in the integral. The same rescaling calculation leads to the
93 following expression

$$\begin{aligned} \mathcal{P}(\tau) &= [(1 + 1/\tau)^{\beta-2} + (1 - 1/\tau)^{\beta-2} - 2] M/2, \tau \neq 1 \\ \mathcal{P}(\tau) &= (2^{\beta-3} - 1) M, \quad \tau = 1 \end{aligned} \quad (18)$$

94 where $M = \int_0^{+\infty} x^{1-\beta}(1 - \cos(2\pi x)) \sin(2\pi x\tau) dx$ and $M > 0$ [7]. The convergence condition
95 requires $1 < \beta < 4$. When $\beta < 2$, one can find that both left and right limits of $\mathcal{P}(1)$ are
96 infinite, but the definition of $\mathcal{P}(1)$ in eq. (17) is finite. Thus $\tau = 1$ is a second type
97 discontinuity point of eq. (17) [8]. It is easy to show that

$$\begin{cases} \mathcal{P}(\tau) < 0, \tau \leq 1 \\ \mathcal{P}(\tau) > 0, \tau > 1 \end{cases} \quad (19)$$

98 It means that $\mathcal{P}(\tau)$ changes its sign from negative to positive when τ is increasing from
99 $\tau < 1$ to $\tau > 1$. In other words the autocorrelation function will take its minimum value at
100 the location where τ is exactly equal to 1. We thus see that $\tau_o(1) = 1$ and hence $\tau_o(\ell) = \ell$
101 (eq. (14)).

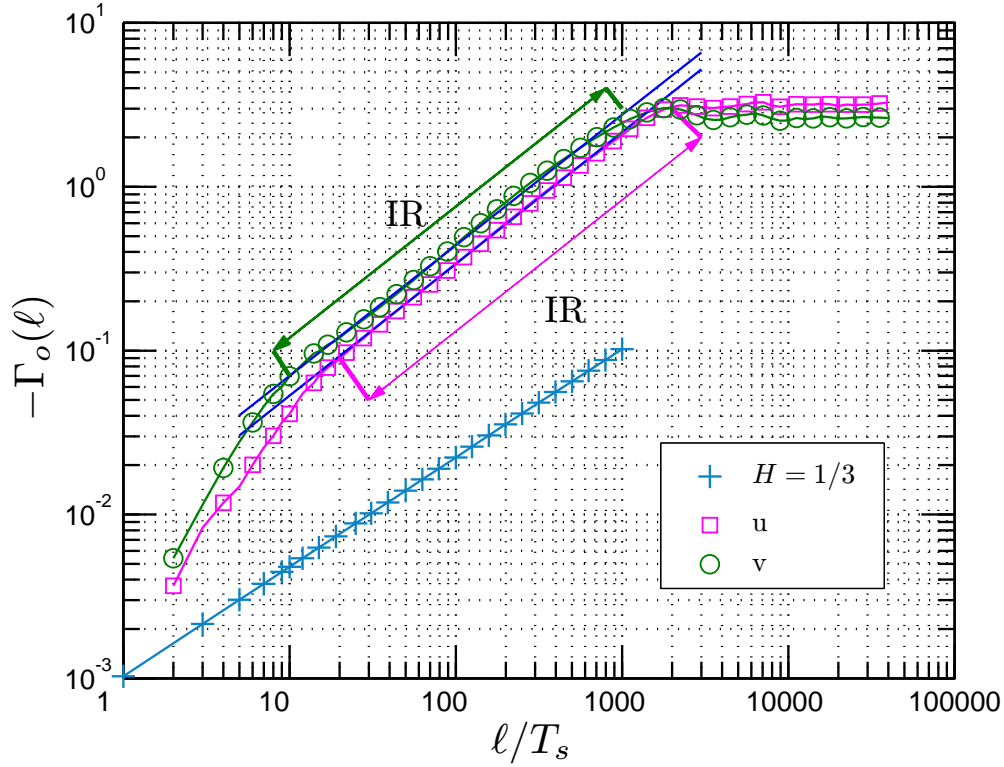


Fig. 6: Representation of the minima value $\Gamma_o(\ell)$ of the autocorrelation function estimated from synthesized fBm time series with $H = 1/3$ (+), and the experimental data for **streamwise (longitudinal)** (\square) and **spanwise (transverse)** (\circ) turbulent velocity components, where the corresponding inertial range is denoted as IR. Power law behaviour is observed with scaling exponent $\beta - 1 = 2/3$ and $\beta - 1 = 0.78 \pm 0.04$ for fBm and turbulent velocity, respectively.

Numerical validation. – There is no analytical solution for eq. (10). It is then solved here by a proper numerical algorithm. We perform a fourth order accurate Simpson rule numerical integration of eq. (10) on range $10^{-4} < f < 10^4$ with $\ell = 1$ for various β with step $\Delta f = 10^{-6}$. We show the rescaled numerical solutions $\Upsilon(\zeta)$ for various β values in fig. 4. Graphically, as what we have proved above, the location $\tau_o(1)$ of the minimum autocorrelation function is exactly equal to 1 when $0 < \beta < 2$.

For the fBm, the autocorrelation function of the increments is known to be the following [9]

$$\Gamma_\ell(\tau) = \frac{1}{2} \{ (\tau + \ell)^{2H} + |\tau - \ell|^{2H} - \tau^{2H} \} \quad (20)$$

where $\tau \geq 0$. We compare the autocorrelation (coefficient) function estimated from fBm simulation (\square , see bellow) with eq. (20) (solid line) in fig. 5, where $\ell = 200$ points. Graphically, eq. (20) provides a very good agreement with numerical simulation. Based on this model, it is not difficult to find that $\Gamma_o(\ell) \sim \ell^{2H}$ when $0 < H < 1$, corresponding to $1 < \beta < 3$, and $\tau_o(\ell) = \ell$ when $0 < H < 0.5$, corresponding to $1 < \beta < 2$. One can find that the validation range of scaling exponent β is only a subset of Wiener-Khinchin theorem.

We then check the power law for the minimum value of the autocorrelation function given in eq. (12). We simulate 100 segments of fractional Brownian motion with length 10^6 data points each, by performing a Wavelet based algorithm [10]. We take db2 wavelet with $H = 1/3$ (corresponding to the Hurst number of turbulent velocity). We plot the estimated minima value $\Gamma_o(\ell)$ (+) of the autocorrelation function in fig. 6. A power law behaviour

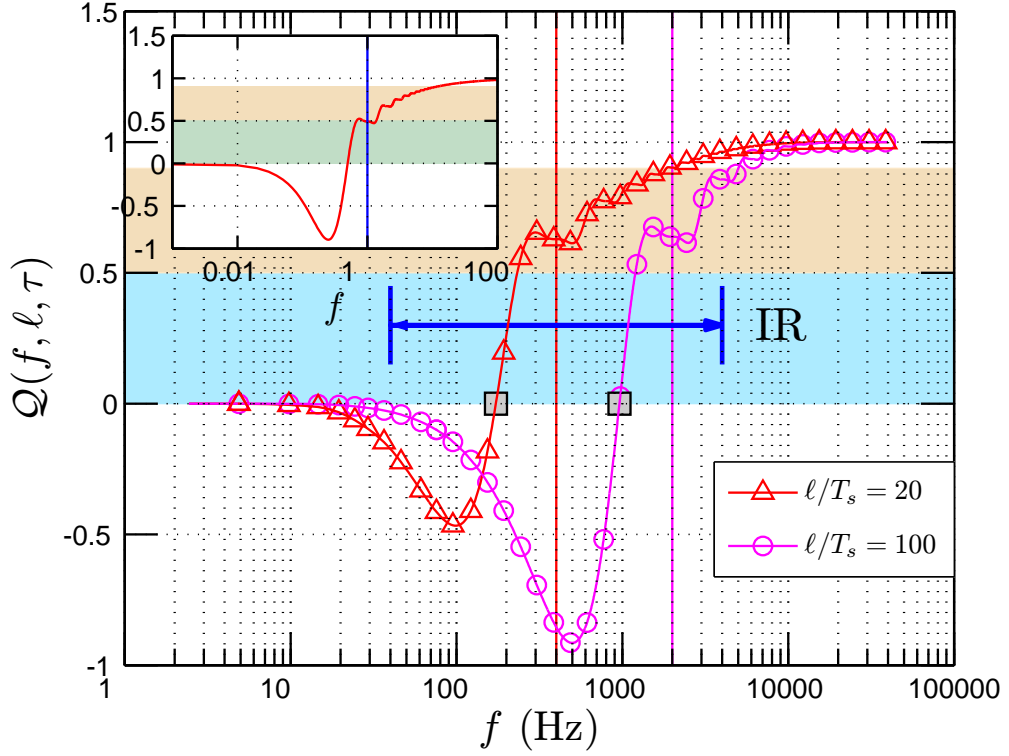


Fig. 7: Cumulative function $\mathcal{Q}(f, \ell, \tau)$ estimated from turbulent experimental data for **spanwise (transverse)** velocity with $\tau = \ell$ in the inertial range, where the numerical solution is shown as inset with $\ell = 1$. The inertial range is denoted as IR. Vertical solid lines demonstrate the corresponding scale in spectral space.

121 is observed with the scaling exponent $\beta - 1 = 2/3$ as expected. It confirms eq. (12) for
 122 fBm. We also plot $\Gamma_o(\ell)$ estimated from turbulent experimental data for both **streamwise**
 123 **(longitudinal)** (\square) and **spanwise (transverse)** (\circ) velocity components in fig. 6, where the
 124 inertial range is marked by IR. Power law is observed on the corresponding inertial range
 125 with scaling exponent $\beta - 1 = 0.78 \pm 0.04$. This scaling exponent is larger than $2/3$, which
 126 may be an effect of intermittency. The exact relation between this scaling exponent with
 127 intermittent parameter should be investigated further in future work. The power law range
 128 is almost the same as the inertial range estimated by Fourier power spectrum. It indicates
 129 that autocorrelation function can be used to determine the inertial range. Indeed, as we
 130 show later, it seems to be a better inertial range indicator than structure function.

131 **Discussion.** – We define a cumulative function

$$\mathcal{Q}(f, \ell, \tau) = \frac{\int_0^f K(f', \ell, \tau) df'}{\int_0^{+\infty} K(f', \ell, \tau) df'} \quad (21)$$

132 where

$$K(f, \ell, \tau) = E_v(f)(1 - \cos(2\pi f\ell)) \cos(2\pi f\tau) \quad (22)$$

133 is the integration kernel of eq. (8). It measures the contribution of the frequency from 0 to
 134 f at given scale ℓ and time delay τ . We are particularly concerned by the case $\tau = \ell$. To
 135 avoid the effects of the measurement noise, see fig. 1, we only consider here the **spanwise**
 136 **(transverse)** velocity. We show the estimated \mathcal{Q} in fig. 7 for two scales $\ell/T_s = 20$ (\circ) and
 137 $\ell/T_s = 100$ (\triangle) in the inertial range, where the **vertical** solid line illustrates the location of

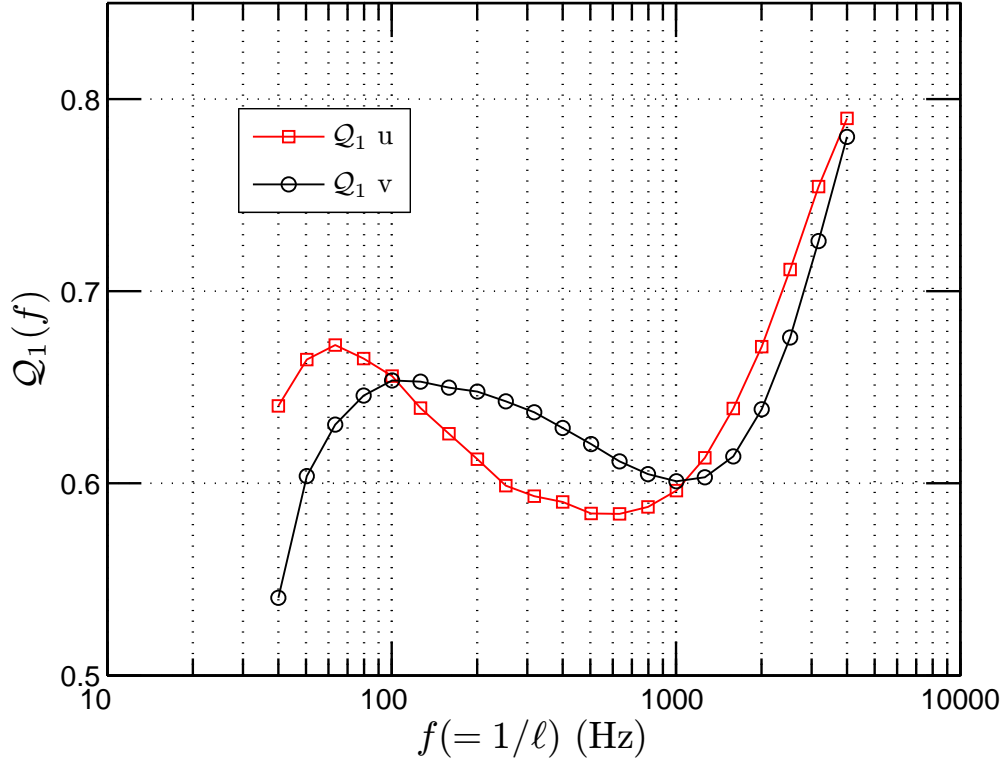


Fig. 8: Cumulative function $Q_1(f)$ estimated from turbulent experimental data for both **streamwise (longitudinal)** and **spanwise (transverse)** velocity with various ℓ . The numerical solution is $Q_1 \simeq 0.5$.

138 the corresponding **time scale** in spectral space. In these experimental curves, the kernel K
 139 given in eq. (22) is computed using the experimental spectrum $E_v(f)$. The corresponding
 140 inertial range is denoted by IR. We also show the numerical solution of eq. (21) with $\ell = 1$
 141 as inset, which is estimated by taking a pure power law $E_v(f) = f^{-\beta}$ in eq. (22). We notice
 142 that both curves cross the line $Q = 0$. We denote f_o such as $Q(f_o) = 0$. It has an advantage
 143 that the contribution from large scale $\ell > 1/f_o$ is canceled by itself. Graphically, in the
 144 inertial range, the distance between f_o and the corresponding scale ℓ is less than 0.3 decade.
 145 The numerical solution indicates that this distance is about 0.3 decade. We then separate
 146 the contribution into a large scale part and a small scale part. We denote the contribution
 147 from the large scale part as $Q_1(f) = Q(1/\ell, \ell, \ell)$. The experimental result is shown in fig. 8
 148 for both **streamwise (longitudinal)** and **spanwise (transverse)** velocity components. The
 149 mean contribution from large scale is found graphically to be 0.64. It is significantly larger
 150 than 0.5, the value indicated by the numerical solution. It means that the autocorrelation
 151 function is influenced more by the large scale than by the small scale.

152 We now consider the inertial range provided by different methods. We replot the cor-
 153 responding compensated spectra estimated **directly** by Fourier power spectrum (solid line),
 154 the second order structure function (\square), the autocorrelation function (\circ) and the Hilbert
 155 spectral analysis (\triangle) [11] in fig. 9 for **streamwise (longitudinal)** velocity. For comparison
 156 convenience, both the structure function and the autocorrelation function are converted
 157 from physical space into spectral space by taking $f = 1/\ell$. For display convenience, these
 158 curves are vertically shifted. Graphically, except for the structure function, the other lines
 159 demonstrate a clear plateau. As we have pointed above, the autocorrelation function is a
 160 better indicator of the inertial range than structure function. We also notice that the inertial

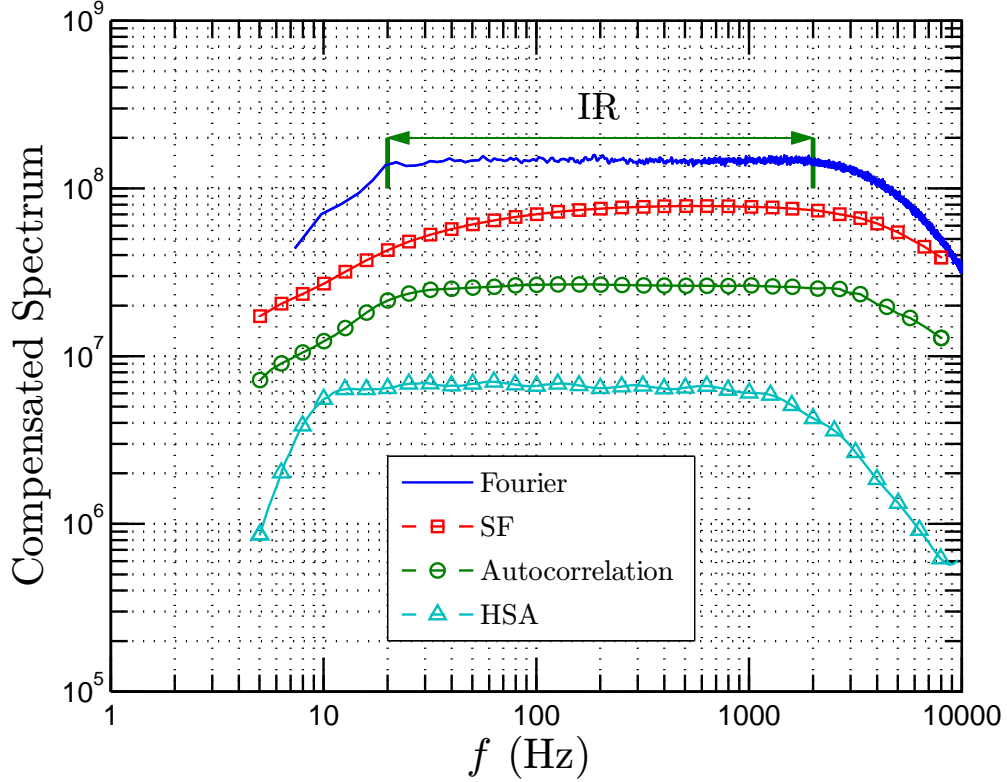


Fig. 9: Comparison of the inertial range for the **streamwise (longitudinal)** velocity. They are estimated **directly** by the Fourier power spectrum, the second order structure function, the Hilbert spectral analysis and the autocorrelation function.

161 range provided by the Hilbert methodology is slightly different from the Fourier spectrum.
 162 This may come from the fact that the former methodology has a very local ability both in
 163 physical and spectral domain [11,12], thus the large scale effect should be constrained. How-
 164 ever, the Fourier analysis requires the stationary of the data, which is obviously not satisfied
 165 by the turbulence data. The result we present here can also be linked with intermittency
 166 property of turbulence: we will present this in future work.

167 **Conclusion.** – In this work, we **considered** the autocorrelation function of the velocity
 168 increment $\Delta u_\ell(t)$ **time series**, where ℓ is a **time scale**. Taking statistical stationary assump-
 169 tion, we **proposed** an analytical model of the autocorrelation function. With this model,
 170 we **proved** analytically that the location of the minimum autocorrelation function is exactly
 171 equal to the separation **time scale** ℓ when the scaling of the power spectrum of the original
 172 variable belongs to the range $0 < \beta < 2$. **In fact, this property was found experimentally**
 173 **to be valid outside the scaling range, but our demonstration here concerns only the scaling**
 174 **range.** This model also suggests a power law expression for the minimum autocorrelation
 175 $\Gamma_o(\ell)$. Considering the cumulative integration of the autocorrelation function **and the second**
 176 **order structure function, it is shown that structure functions are strongly influenced by the**
 177 **large-scale, it was shown that the autocorrelation function is influenced more by the large**
 178 **scale part.** Finally we argue that the autocorrelation function is a better indicator of the iner-
 179 tial range than second order structure function. **These results have been illustrated using**
 180 **fully developed turbulence data; however, they are of more general validity since we only**
 181 **assumed that the considered time series is stationary and possesses scaling statistics.**

* * *

182 This work is supported in part by the National Natural Science Foundation of China
183 (No.10772110) and the Innovation Foundation of Shanghai University. Y.H. is financed
184 in part by a Ph.D. grant from the French Ministry of Foreign Affairs. We thank Nicolas
185 Perpète for useful discussion. Experimental data have been measured in the Johns Hopkins
186 University's Corrsin wind tunnel and are available for download at C. Meneveau's web page:
187 <http://www.me.jhu.edu/~meneveau/datasets.html>.

188 REFERENCES

- 189 [1] KOLMOGOROV A. N., *Dokl. Akad. Nauk SSSR* , **30** (1941) 299.
190 [2] MONIN A. S. and YAGLOM A. M., *Statistical fluid mechanics* (MIT Press Cambridge, Mass)
191 1971.
192 [3] FRISCH U., *Turbulence: the legacy of AN Kolmogorov* (Cambridge University Press) 1995.
193 [4] ANSELMET F., GAGNE Y., HOPFINGER E. J. and ANTONIA R. A., *J. Fluid Mech.* , **140** (1984)
194 63.
195 [5] KANG H., CHESTER S. and MENEVEAU C., *J. Fluid Mech.* , **480** (2003) 129.
196 [6] PERCIVAL D. and WALDEN A., *Spectral Analysis for Physical Applications: Multitaper and*
197 *Conventional Univariate Techniques* (Cambridge University Press) 1993.
198 [7] SAMORODNITSKY G. and TAQQU M., *Stable Non-Gaussian Random Processes: stochastic mod-*
199 *els with infinite variance* (Chapman & Hall) 1994.
200 [8] MALIK S. and ARORA S., *Mathematical Analysis* (John Wiley & Sons Inc) 1992.
201 [9] BIAGINI F., HU Y., OKSENDAL B. and ZHANG T., *Stochastic calculus for fractional Brownian*
202 *motion and applications* (Springer Verlag) 2008.
203 [10] ABRY P. and SELLAN F., *Appl. Comput. Harmon. Anal.* , **3** (1996) 377.
204 [11] HUANG Y., SCHMITT F. G., LU Z. and LIU Y., *Europhys. Lett.* , **84** (2008) 40010.
205 [12] HUANG Y., SCHMITT F. G., LU Z. and LIU Y., *Traitement du Signal (in press)* , (2009) .